

Journal of Applied Fluid Mechanics, Vol. 4, No. 4, pp. 15-21, 2011.
Available online at www.jafmonline.net, ISSN 1735-3572, EISSN 1735-3645.
DOI: 10.36884/jafm.4.04.11941



Natural Convection Heat and Mass Transfer in the Boundary Layer along a Vertical Cylinder with Opposing Buoyancies

M. Si Abdallah^{1†} and B. Zeghmami²

¹ *Laboratory of Physics Energy, University of Mentouri, Constantine 25000, Algeria*

² *M.E.P.S-G.M.E. Laboratoire de Mathématiques et Physique des Systèmes, Université de Perpignan Via Domitia, France*

†Corresponding Author Email: s_maayouf@yahoo.fr

(Received January 23, 2009; accepted July 15, 2010)

ABSTRACT

The effects of opposing buoyancies on natural convection heat and mass transfer in the boundary layer over a vertical cylinder immersed in a quiescent Newtonian fluid are presented in this paper. The surface of the cylinder is maintained at a constant temperature and concentration. The homotopic transformation is proposed to transform the physical domain into a flat plate. The boundary layer equations and the boundary conditions are solved numerically using an implicit finite difference scheme and the Gauss-Seidel algorithm. The buoyancy ratio N , Prandtl number Pr and Schmidt number Sc are important parameters for this problem. The numerical results for $Pr=Sc$ and $Pr \neq Sc$, including the velocity, temperature, concentration fields and the Nusselt number as well as the Sherwood number along the surface of the cylinder are discussed for aiding and opposing buoyancies. Results show that the Nusselt (Sherwood) number increases with positive or negative buoyancies ratio N ($N=Gr_c/Gr_t$). Moreover, for opposing flows with $Sc < Pr$, the flow is completely downward, the thickness of the concentration layer is larger than that of the thermal layer. For $Pr < Sc$, the velocity are weak and the thermal layer thickness is much larger.

Keywords: Free convection, Boundary layer, Buoyancy force, Vertical cylinder, Heat transfer, Mass transfer.

NOMENCLATURE

C	concentration	u, v	velocity components in x and y direction
C	dimensionless concentration	U, V	dimensionless velocity components
D	diffusion coefficient of the species	x, y	Cartesian coordinates
G	gravitational acceleration	X, Y	dimensionless Cartesian coordinates
Gr_t	thermal Grashof number	α	thermal diffusivity
Gr_c	species Grashof number	β_t	thermal expansion coefficient
K	thermal conductivity of the fluid	β_c	species expansion coefficient
L	length of the cylinder	μ	dynamic viscosity
N	buoyancy ratio	ν	kinematic viscosity
Nu_L	mean Nusselt number	θ	dimensionless temperature
Nu_x	local Nusselt number	ξ, η	dimensionless coordinates in the computational domain
Pr	Prandtl number	x, y	derivation with respect to x and y direction
r	radius of the cylinder	w	surface condition
r^*	dimensionless radius	∞	reference
Sc	Schmidt number		
Sh_L	mean Sherwood number		
Sh_x	local Sherwood number		
T	temperature		

1. INTRODUCTION

Heat and mass transfer along a surface have received considerable attention in recent years because of their importance in wide range of scientific field such as

biology, oceanography, astrophysics, geology, chemical processes and crystal-growth techniques as those reported by Fournier (1990), Rudels *et al.* (1999),

Marcoux *et al.* (1999), Mamou (2003), and Markus (2004).

In nature, the free convection currents caused by differences of the temperature, the flow is also affected by the differences in material constitution, for example, in atmospheric flows there exist differences in H₂O concentration and hence the flow is affected by such concentration difference. In many engineering applications, the foreign gases are injected. This causes a reduction in wall shear stress, the mass transfer conductance or the rate of heat transfer. Usually, H₂O, CO₂, etc are the foreign gases, which are injected in the air flowing past bodies. The effects of foreign mass, also know as diffusing species concentration were studied under different conditions by Somers (1956), Mathers *et al.* (1956), and others either by integral method or by asymptotic analysis.

Previous studies of natural convection heat and mass transfer have focused mainly on a flat plate or regular ducts. Somers (1956), Mather *et al.* (1957), and Gill *et al.* (1965) analyzed the same problem of simultaneous heat transfer and double diffusion on a vertical surface with different situations or different numerical schemes. Adams and Fadden (1966) experimentally studied the free convection with opposing body force. Bottemanne (1971) has considered simultaneous heat and mass transfer by free convection along a vertical flat plate only for steady state theoretical solutions with Pr= 0.71 and Sc=0.63. Gebhart and Pera (1971) made a general formulation of the vertical two-dimensionless boundary layer flows.

Moreover, these results were extended to flows about horizontal surfaces by Pera and Gebhart (1972). Callahan and Marner (1976) studied the free convection with mass transfer on a vertical flat plate with Pr=1 and a realistic range of Schmidt number. Chen and Yuh (1979) investigated the effects of inclination of flat plate on the combined heat and mass transfer in natural convection. Chen and Yuh (1980) presented local non similarity solution for natural convection along a vertical cylinder. Chen *et al.* (1980) studied the mixed convection with combined buoyant mechanism along vertical and inclined plates. Jang and Chang (1988) studied the problem of buoyancy-induced inclined boundary flows in a porous medium resulting from combined heat and mass buoyancy effects. Mahajan and Angivasa (1993) studied the natural convection along a heated surface with opposing buoyancies. Results show that boundary layer solutions do not yield accurate solutions for natural convection flows with opposing buoyancies. Moreover, the heat and mass transfer rates follow complex trends depending on the buoyancy ratio. Ching-Yang (2000) analysed the free thermal and mass transfer near a vertical wavy surface with constant wall temperature and concentration in a porous medium. The results obtained show that increasing the buoyancy ratio tends to increase both the Nusselt and Sherwood numbers. Kefeng and Wen-Qiang (2006) numerically analyzed the magnitude of the buoyancy ratio N on the double-diffusive convection in a vertical cylinder with radial temperature and axial solutal gradients for different values of Gr, Pr and Sc.

The aim of the present work is to examine numerically the laminar natural convection heat and mass transfer along a vertical cylinder with opposing buoyancies. The boundary layer equations and the boundary conditions are solved numerically using an implicit finite difference scheme and the Gauss-Seidel algorithm. The numerical results for different numbers of Pr and Sc as well as for different buoyancy ratio N (N > 0 and N < 0) on the characters of the flow, heat and mass transfer rates are investigated in detail.

2. MODEL DESCRIPTION

It is considered a vertical cylinder as shown schematically in Fig.1. The surface of this cylinder is maintained at a uniform temperature T_w and concentration c_w different than the ambient medium one T_∞ and c_∞ . The buoyancy forces induced by theses temperatures and concentration give rise to the flow. The origin of the Cartesian coordinates system (x,y) is placed at the leading edge of the surface. The u and v are the velocity components in the x and y direction respectively. The fluid is assumed to have constant physical proprieties except for the density variation in the buoyancy term of the momentum equation.

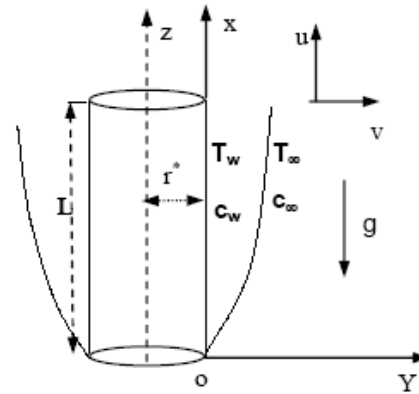


Fig. 1. Physical model and coordinates system

3. GOVERNING EQUATIONS

The governing equations for a steady, laminar and incompressible flow in the boundary layer along a vertical cylinder with Boussinesq approximation may be written as:

Continuity equation

$$u \frac{\partial(u)}{\partial x} + v \frac{\partial(v)}{\partial y} = 0 \quad (1)$$

Momentum equation

$$u \frac{\partial u}{\partial x} + v \frac{\partial u}{\partial y} = -\frac{1}{\rho} \frac{\partial p}{\partial x} + \nu \left(\frac{\partial^2 u}{\partial x^2} + \frac{\partial^2 u}{\partial y^2} \right) + g \beta_T (T - T_\infty) + g \beta_c (c - c_\infty) \quad (2)$$

$$u \frac{\partial v}{\partial x} + v \frac{\partial v}{\partial y} = -\frac{1}{\rho} \frac{\partial p}{\partial y} + \nu \left(\frac{\partial^2 v}{\partial x^2} + \frac{\partial^2 v}{\partial y^2} \right) \quad (3)$$

Energy equation

$$\left(u \frac{\partial T}{\partial x} + v \frac{\partial T}{\partial y} \right) = \frac{k}{\rho c_p} \left(\frac{\partial^2 T}{\partial x^2} + \frac{\partial^2 T}{\partial y^2} \right) \quad (4)$$

Concentration equation

$$\left(u \frac{\partial c}{\partial x} + v \frac{\partial c}{\partial y} \right) = D \left(\frac{\partial^2 c}{\partial x^2} + \frac{\partial^2 c}{\partial y^2} \right) \quad (5)$$

The appropriate boundary conditions for the problem are:

$$\begin{aligned} \text{At the surface, } y=f(x): \quad & u=0, v=0, T= T_w, c=c_w \\ y \rightarrow \infty: \quad & u=0, T= T_\infty, c=c_\infty \end{aligned} \quad (6)$$

In no-dimensionless, the governing equations, the following variables were introduced

$$\begin{aligned} X &= \frac{x}{L}; \quad Y = \frac{y}{L} Gr^{1/4}; \quad r^* = \frac{r}{L}; \\ U &= \frac{L}{\nu Gr^{1/2}} u; \quad V = \frac{L}{\nu Gr^{1/4}} v; \\ P &= \frac{\rho L^2}{\mu^2 Gr} p, \quad Gr = \frac{g \beta_T (T_w - T_\infty)}{\nu^2} L^3 \\ \theta &= \frac{T - T_\infty}{T_w - T_\infty}; \quad C = \frac{c - c_\infty}{c_w - c_\infty} \end{aligned} \quad (7)$$

For the current problem, after ignoring the small order terms in Gr and the pressures $\partial p/\partial x$, $\partial p/\partial y$. With the no-dimensionless variables (7), Eqs. (1)-(5) become

$$\frac{\partial(r^*U)}{\partial X} + \frac{\partial(r^*V)}{\partial Y} = 0 \quad (8)$$

$$U \frac{\partial U}{\partial X} + V \frac{\partial U}{\partial Y} = \frac{\partial^2 U}{\partial Y^2} + \theta + NC \quad (9)$$

$$U \frac{\partial \theta}{\partial X} + V \frac{\partial \theta}{\partial Y} = \frac{1}{Pr} \frac{\partial^2 \theta}{\partial Y^2} \quad (10)$$

$$U \frac{\partial C}{\partial X} + V \frac{\partial C}{\partial Y} = \frac{1}{Sc} \frac{\partial^2 C}{\partial Y^2} \quad (11)$$

$$\text{Where, } Pr = \frac{\mu C_p}{k}; \quad Sc = \frac{\mu}{\rho D}$$

Moreover, the above equations are subject to the following boundary conditions:

$$\begin{aligned} Y=0: \quad & U = 0; \quad V = 0; \quad \theta = 1; \quad C = 1 \\ Y \rightarrow \infty: \quad & U = 0; \quad V = 0; \quad \theta = 0; \quad C = 0 \end{aligned} \quad (12)$$

3.1 Coordinate Transformation

In order to avoid the non-uniformity of the mesh spacing in the vicinity of the outer surface of the cylinder, the physical domain is transformed into a straight line using the following transformation (Yao 1983):

$$\begin{aligned} f(X, Y) &\rightarrow f(\xi, \eta) \\ x = \xi; \quad \eta &= \frac{Y}{(4\xi)^{1/4}} \end{aligned} \quad (13)$$

In the new coordinate system (0, ξ , η) the Eqs. (6-9) became:

$$\frac{\partial U}{\partial \xi} + \eta_x \frac{\partial U}{\partial \eta} + \frac{\partial V}{\partial \eta} = 0 \quad (14)$$

$$U \frac{\partial U}{\partial \xi} + (\eta_x U + V \eta_y) \frac{\partial U}{\partial \eta} = (\eta_y)^2 \frac{\partial^2 U}{\partial \eta^2} + \theta + N.C \quad (15)$$

$$U \frac{\partial \theta}{\partial \xi} + (\eta_x U + V \eta_y) \frac{\partial \theta}{\partial \eta} = \frac{\eta_y^2}{Pr} \frac{\partial^2 \theta}{\partial \eta^2} \quad (16)$$

$$U \frac{\partial C}{\partial \xi} + (\eta_x U + V \eta_y) \frac{\partial C}{\partial \eta} = \frac{\eta_y^2}{Sc} \frac{\partial^2 C}{\partial \eta^2} \quad (17)$$

Where, η_x and η_y are the first derivative of the variable η to x and y respectively.

The corresponding boundary conditions are:

$$\begin{aligned} \eta = 0; \quad & U = V = 0; \quad \theta = 1; \quad C = 1 \\ \eta \rightarrow \infty: \quad & U = 0; \quad \theta = 0; \quad C = 0 \end{aligned} \quad (18)$$

The local Nusselt number and the local Sherwood number are defined in the (0, ξ , η) coordinate system as:

$$Nu_x = - \left(\frac{Gr}{4\xi} \right)^{1/4} \left(\frac{\partial \theta}{\partial \eta} \right)_{\eta=0} \quad (19)$$

$$Sh_x = - \left(\frac{Gr_c}{4\xi} \right)^{1/4} \left(\frac{\partial C}{\partial \eta} \right)_{\eta=0} \quad (20)$$

The dimensionless average rates of heat and mass transfer along the surfer of the cylinder are expressed by the mean Nusselt and Sherwood numbers, respectively

$$Nu_L / Gr^{1/4} = - \frac{1}{L} \int_0^L \frac{1}{(4\xi)^{1/4}} \left[\frac{\partial \theta}{\partial \eta} \right]_{\eta=0} d\xi \quad (21)$$

$$Sh_L / Gr_c^{1/4} = - \frac{1}{L} \int_0^L \frac{1}{(4\xi)^{1/4}} \left[\frac{\partial C}{\partial \eta} \right]_{\eta=0} d\xi \quad (22)$$

4. NUMERICAL METHOD

In this work, a marching finite difference schemes was used to discretize the coupled Eqs. (8)-(11) for U, V, θ and C. Moreover, grid independency checks were made. Some of the calculations were tested using (400x350) nodes in the X and Y directions respectively but no significant improvement over (220x190) grid points was found. The algebraic systems of equations are solved using Gauss-Seidel algorithm with a relaxation coefficient equal to 0.1 for the variables U, V and to 0.2 for θ and C. During the program test, the convergence criterion used was $|\Phi^{k+1} - \Phi^k| / \Phi^{k+1} |_{\max} \leq 10^{-5}$, where Φ^k and Φ^{k+1} are the values of the k^{th} and $(k+1)^{\text{th}}$ iterations of U, V, θ and C. Furthermore, the numerical scheme used in this work is checked. Our computational results for aiding and opposing buoyancies were compared with the experimental data (Pr=0.7, Sc=2.23) for opposing flow which were obtained for a vertical surface by Adams (1966) and with the numerical results obtained by Mahajan (1993).

5. RESULTS AND DISCUSSION

The controlling parameters of the fluid flow and heat and mass transfer rates for the laminar natural convection in the boundary layer along the surface of the vertical cylinder are Prandtl number Pr, Sherwood number Sc and buoyancy ratio N ($N = Gr_c/Gr$). The detailed numerical results of velocity, temperature and concentration fields are presented. Hence, the inadequacies of the boundary layer analysis are specified. Moreover, we present comprehensive results of Nusselt and Sherwood numbers for some values of Pr and Sc.

We first compare our computational results (Nu and Sh) with the experimental data (Pr=0.7, Sc=2.23) for opposing flow which were obtained for a vertical

surface by (Adams and McFadden 1966) as well as with the numerical results obtained by (Mahajan and Angirasa 1993).

Table 1 Comparison of Nu and Sh numbers for a vertical surface for $N=-0.43$

	Nu	Sh
Present work	25.24	41.30
(Adams and Mc.Fadden 1966)	24.38	42.10
(Mahajan and Angirasa 1993)	23.03	41.44

The comparison is presented in Table 1. We observe that the agreement between our numerical results and those obtained by the authors is very good. These results are just the same as for a vertical flat plate because in our computational, the radius r_0 of the cylinder is considered very small than its length L .

5.1 Boundary Layer Analysis

The velocity profiles for $Pr=0.7$, $Sc=5$ ($Pr < Sc$) and for a different values of negative N are presented in Fig. 2. As shown in this figure, while $N=-0.5$, the U velocity is positive and the flow upward. This suggests that for this values of N , although the boundary layer analysis predicts a reasonably solution. Moreover, for $N < -0.5$, the U velocity is negative for $\eta < 0.2$ and positive for $\eta > 0.2$.

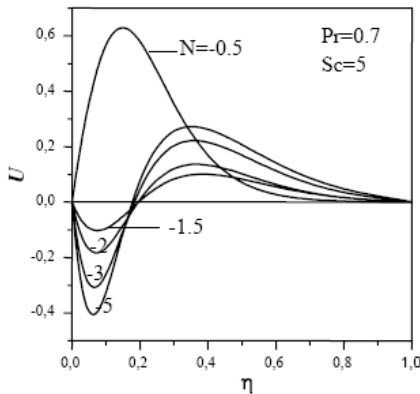


Fig. 2. Velocity profiles for different values of N for $Pr < Sc$

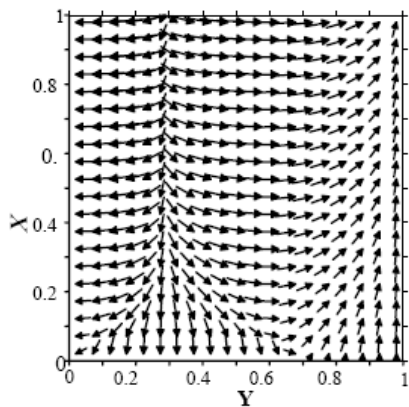


Fig. 3. Streamfunction contours for $N=-2$ and for $Pr=0.7$, $Sc=5$ ($Pr < Sc$)

Figure 3 shows that the flow reversal near the surface and exaggerates the magnitude of the upward velocities

and this can not be accounted as a boundary layer type flow. In Figs. 4 and 5, for $Pr=Sc=0.7$ and for $Pr > Sc$, when $N < -0.5$, the mass buoyancy is greater than the thermal buoyancy, hence the U velocity is negative and the flow is fully reversed as observed in Figs. 6 and 7. It is worth noting that for $N=-1$ and for $Pr=Sc$, the flow is steady; this is because in this case, the two buoyancies are equal to and oppose each other.

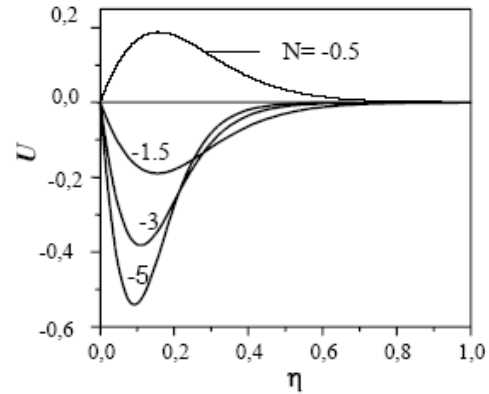


Fig. 4. Velocity profiles for different values of N ($Pr=Sc=0.7$)

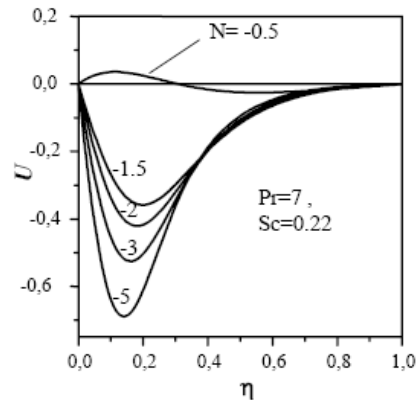


Fig. 5. Velocity profiles for different values of N ($Pr > Sc$)

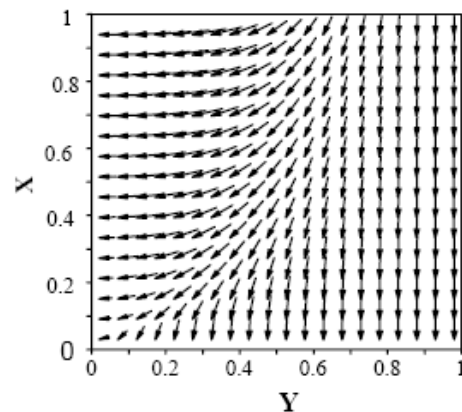


Fig. 6. Stream function contours for $N=-2$, ($Pr=Sc=0.7$)

5.2 Nusselt and Sherwood Number

The variation of the average Nusselt (Sherwood) number for $Pr=Sc$, $Pr < Sc$ and for $Pr > Sc$ with positive and negative buoyancy ration N is presented in Figs. 8, 9 and 10.

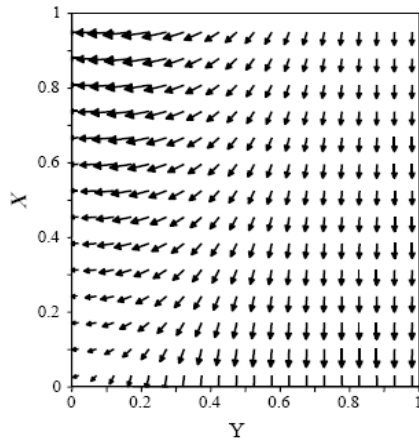


Fig. 7. Stream function contours for $N = -2$, $Pr = 7$, $Sc = 0.22$ ($Pr > Sc$)

From these figures, it can be seen that increasing of positive or negative N leads to increase both the average Nusselt number and the average Sherwood number for all cases of Pr and Sc . In the case of $Pr = Sc = 0.7$, Fig. 8 illustrates the effect of the buoyancy ratio N for the Nusselt and the Sherwood numbers. It is seen that the N - Nu or N - Sh curve is symmetric about $N_{min} = -1$ and the heat transfer is the same as the mass transfer where the thicknesses of the thermal and concentration layers are equal (not shown). For $Pr = 0.7$ and $Sc = 5$ ($Pr < Sc$), Fig. 9 shows that the mass transfer is greater than the heat transfer, this is because the thermal layer thickness is more important than the concentration layer thickness as shown in Fig. 11.

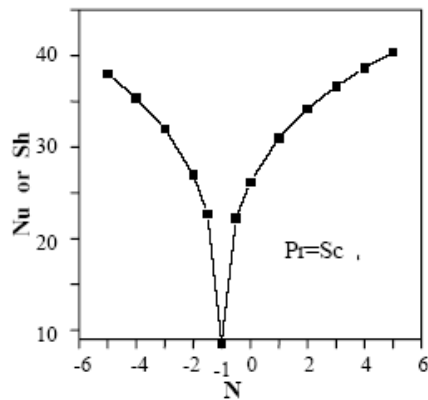


Fig. 8. Nusselt (Sherwood) number for $Pr = Sc = 0.7$

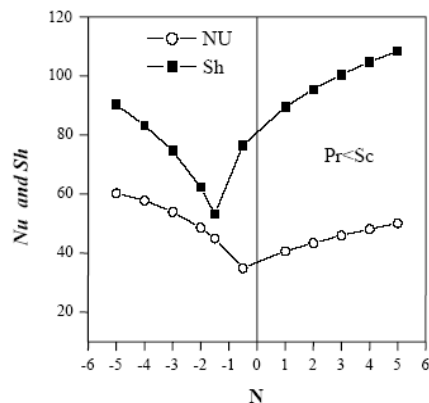


Fig. 9. Nusselt and Sherwood numbers for $Pr = 0.7$, $Sc = 5$

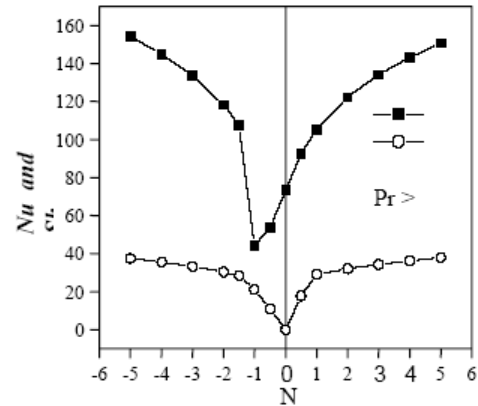


Fig. 10. Nusselt and Sherwood numbers for $Pr = 7$, $Sc = 0.22$

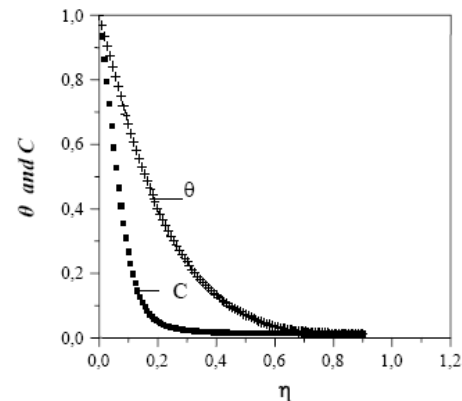


Fig. 11. Temperature and Concentration profiles for $Pr < Sc$

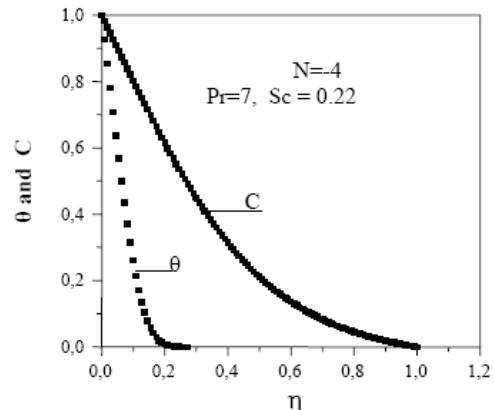


Fig. 12. Temperature and Concentration Profiles for $Pr > Sc$

This can be explained from Fig. 12, the thermal layer thickness is much smaller which leads to reduce the thermal conduction between the fluid and the surface of the cylinder. Consequently, It should be noted that for $Pr \neq Sc$, The Nu - N and Sh - N curves are not symmetric (see Figs. 9 and 10). This is explained from the unequal thicknesses of the thermal and concentration layers (Figs. 11 and 12).

5.3 Correlation

A correlation has been made from Figs. 9 and 10 for the mean Nusselt (Sherwood) number as a function

of the buoyancy ratio N which are found that they depend to the Pr and Sc numbers;

For $N \geq -1$

$$Nu_L = A_2 + Pr \frac{A_2 - A_1}{1 + e^{(N - N_0)/DN}}$$

$$Sh_L = A_2 + Sc \frac{A_2 - A_1}{1 + e^{(N - N_0)/DN}}$$

Where;

$$A_1 = 147.35; A_2 = 166.52; N_0 = -0.95; DN = 3.27$$

For $N < -1$;

$$A_1 = -857.85; A_2 = 1002.85; N_0 = 1, DN = 1.$$

6. CONCLUSION

In this work, the free convection heat and mass transfer in the boundary layer with opposing buoyancies along a vertical cylinder with a constant surface temperature and concentration has been analyzed numerically. The physical domain is transformed using a homotopic transformation into a straight line. The effects of the positive and negative buoyancy ratio N , Prandtl number Pr and Schmidt number Sc on heat and mass transfer in the boundary layer have been studied in detail. Brief summaries of the major results are listed in the following:

- Finite difference solutions of the boundary layer equations give accurate solutions. Our numerical results agree very well with the velocity fields as well as with the Nusselt and Sherwood number with the known results for a vertical surface with aiding and opposing buoyancies.
- The heat and mass transfer rates submit for a complex changes with positive and negative N . From a minimum at a particular value of negative N which is a function of Pr and Sc , increasing or decreasing N leads to increase both Nu and Sh numbers.
- Boundary layer solutions do not yield exact solutions for free convection flows with opposing buoyancies for $Pr < Sc$. In this case, the flow reversal near the surface and exaggerates the magnitude of the upward velocities.

REFERENCES

Adams, J.A. and P.W. McFadden (1966). Simultaneous heat and mass transfer in free convection with opposing body forces. *AIChE, Journal*, 12, 642-647.

Bottemanne, F.A. (1971). Theoretical solution of simultaneous heat and mass transfer by free convection about a vertical flat plate. *Applied Scientific Research* 25, 137-149.

Callahan, G.D. and W.J. (1976). Transient free convection with mass transfer on an isothermal vertical flat plate. *International Journal of Heat and Mass Transfer* 19, 165-174.

Chen, T.S. and C.F. Yuh (1979). Combined heat and mass transfer in natural convection on inclined surfaces. *Numerical Heat Transfer* 2, 233-250.

Chen T.S. and C.F. Yuh (1980). Combined heat and mass transfer in natural convection along a vertical cylinder. *International Journal of Heat and Mass Transfer* 23, 451-461.

Chen, T.S, C.F. Yuh and A. Motalgolon (1980). Combined heat and mass transfer in mixed convection along a vertical and inclined plates. *International Journal of Heat and Mass Transfer* 23, 527-537. Somers, E. (1956). Theoretical considerations of combined thermal and mass transfer from a flat plate. *ASME, Journal of Applied Mechanical* 23, 295-301.

Ching-Yang Cheng (2000). Natural convection heat and mass transfer near a vertical wavy surface with constant wall temperature and concentration in a porous medium. *International Communication of Heat and Mass Transfer* 27(8), 1143-1154.

Fournier, R.O. (1990). Double-diffusive convection in geothermal systems: the Salton Sea. *California, Geothermal System as a likely candidate Geothermics* 19(6), 481-496.

Gebhart, B., L. Pera (1971). The nature of vertical natural convection flows resulting from the combined buoyancy effects of thermal and mass diffusion. *International Journal of Heat and Mass Transfer* 14, 2025-2050.

Gill, W.N., E.D. Casal and D.W. Zeh (1965). Binary diffusion and heat transfer in laminar free convection boundary layers on a vertical plate. *International Journal of Heat and Mass Transfer* 8, 1135-1151.

Jang, J.Y., and W.J. Chang (1988). Buoyancy-induced inclined boundary layer flow in a saturated porous medium resulting from combined heat and mass buoyancy effects. *International Communication Heat and Mass Transfer* 15, 17-30.

Kefeng, Shi. and Lu. Wen-Qiang (2006). Time evolution of double-diffusion convection in a vertical cylinder with radial temperature and axial solutal gradients. *International Journal of Heat and Mass Transfer* 49, 995-1003.

Mahajan, R.L. and D. Angirasa (1993). Combined heat and mass transfer by natural convection with opposing buoyancies. *Journal of Heat Transfer* 115, 606-611.

Mamou, M. (2003). Stability analysis of the perturbed rest state and of the finite amplitude steady double-diffusion convection in a shallow porous enclosures. *International Journal of Heat and Mass Transfer* 46(12), 2263-2277.

Marcoux, M., M.C. Charrier-Mojtabi and M. Azaiez (1999). Double diffusive convection in an annular

vertical porous layer. *International Journal of Heat and Mass Transfer* 42(13), 2313–2325.

Markus, M. (2004). Double-diffusive convection: a simple demonstration. *Journal of Chemical Education* 81(4), 526–529.

Mather, W.G., A.J. Madden and E.L. Piret (1957). Simultaneous heat and mass transfer in free convection. *Industrial Engineering Chemical* 49, 961-968.

Pera, L. and B. Gebhart (1972). Natural convection flows adjacent to horizontal surfaces resulting from the combined buoyancy effects of thermal and mass diffusion. *International Journal of Heat and Mass Transfer* 15, 269-278.

Rudels, B., G. Björk, R.D. Muench and U. Schauer (1999). Double-diffusive layering in the Eurasian basin of the arctic ocean. *Journal of Marine Systems* 21, 3–27.

Yao, L.S. (1983). Natural convection along a wavy surface. *Journal of Heat Transfer* 105, 465-468.